Paleomagnetism and geobarometry of the Granite Mountain batholith, Yukon: Minimal geotectonic motion of the Yukon-Tanana Terrane relative to North America

P.J.A. McCausland[1]
Earth Sciences, University of Western Ontario[1]

D.T.A. Symons[2]
Earth Sciences, University of Windsor[2]

C.J.R. Hart[3]
Yukon Geology Program

W.H. Blackburn[2]
Earth Sciences, University of Windsor[2]

McCausland, P.J.A., Symons, D.T.A., Hart, C.J.R. and Blackburn, W.H., 2002. Paleomagnetism and geobarometry of the Granite Mountain batholith, Yukon: Minimal geotectonic motion of the Yukon-Tanana Terrane relative to North America. *In:* Yukon Exploration and Geology 2001, D.S. Emond, L.H. Weston and L.L. Lewis (eds.), Exploration and Geological Services Division, Yukon, Indian and Northern Affairs Canada, p. 163-177.

ABSTRACT

Paleomagnetic and geobarometric results are reported here for the Early Jurassic Granite Mountain batholith, an ~600 km^2 granodiorite intrusion in the Yukon-Tanana Terrane. Paleomagnetic analyses of 331 specimens from 24 sites yield magnetite-borne characteristic remanent magnetization (ChRM) directions. Eight northerly and westerly sites display a mean direction **A** (D=337, I=69°; α_{95}=7.6°, k=54). Another 11 sites appear to be lightning-struck, or exhibit unstable remanence, and 3 sites in a fault-bounded block to the southeast carry an anomalous northeast upwards ChRM direction **B**. Two sites in a Cretaceous andesite porphyry dyke and its contact zone give a westerly, steep-down ChRM direction, **C**. Aluminum-in-hornblende geobarometry at 10 sites defines emplacement depths of ~16 km in the north and west, and ~19 km in the southeast. The batholith has probably not been significantly tilted since its emplacement, but it may be subdivided into two separate intrusive phases or structural blocks that have experienced differential uplift. Ambient temperatures at 16-19 km were too high for magnetite to record an enduring remanence, so the observed ChRMs likely record uplift of the batholith through ~15 km depth, at 180-170 Ma. Both **A** and **C** ChRM directions are similar to those expected for Early Jurassic and Late Cretaceous reference poles, respectively, suggesting that the Yukon-Tanana Terrane is not far-traveled with respect to cratonic North America since Early Jurassic time.

RÉSUMÉ

Les auteurs rapportent des résultats paléomagnétiques et géobarométriques relatifs au batholite de Granite Mountain, datant du Jurassique précoce, qui est une intrusion de granodiorite d'environ 600 km^2 dans le terrane de Yukon-Tanana. Les analyses paléomagnétiques effectuées sur 331 échantillons provenant de 24 sites fournissent des directions de magnétisation rémanente caractéristique (ChRM) dans la magnétite. Huit sites au nord et à l'ouest présentent une direction moyenne **A** (D=337, I=69°; α_{95}=7,6°, k=54). Onze autres sites semblent avoir été frappés par la foudre ou présenter une rémanence instable, et trois sites dans un bloc limité par des failles au sud-est présentent une direction de ChRM **B** anormale ascendante nord-est. Deux sites, situés dans un dyke de porphyre d'andésite datant du Crétacé ainsi que dans la zone de contact du dyke, présentent une direction de ChRM **C** plongeant abruptement vers l'ouest. Dans dix sites, la géobarométrie de l'aluminium dans la hornblende indique que la profondeur de mise en place est d'environ 16 km, au nord et à l'ouest, et d'environ 19 km, au sud-est. Le batholite ne s'est probablement pas incliné de façon significative depuis sa mise en place, mais il peut être subdivisé en deux phases intrusives ou blocs structuraux distincts, qui ont subi un soulèvement différentiel. Entre 16 et 19 km, les températures ambiantes étaient trop élevées pour que la magnétite présente une rémanence durable; par conséquent, les directions de ChRM observées remontent probablement à l'époque du soulèvement du batholite à environ 15 km de profondeur, il y a entre 180 et 170 millions d'années. Les directions de ChRM **A** et **B** sont toutes deux similaires à celles prévues respectivement pour les pôles de références au Jurassique précoce et au Crétacé tardif, ce qui suggère que le terrane de Yukon-Tanana ne s'est pas déplacé sur une grande distance par rapport à l'Amérique du Nord cratonique depuis le Jurassique précoce.

[1]*Earth Sciences, University of Western Ontario, London, Ontario, Canada N6A 5B7, pjam@julian.uwo.ca*

[2]*Earth Sciences, University of Windsor, Windsor, Ontario N9B 3P4, dsymons@uwindsor.ca, blackbu@uwindsor.ca*

[3]*craig.hart@gov.yk.ca*

INTRODUCTION

Paleomagnetic research conducted in the Northern Cordillera with the LITHOPROBE-SNORCLE transect provides regional-scale constraints upon possible past terrane motions. Paleomagnetic results from the Stikine and Cache Creek terranes have refined estimates of the timing and magnitude of their net poleward motion and clockwise rotation with respect to North America (Harris et al., 1999; Symons et al., 2000a).

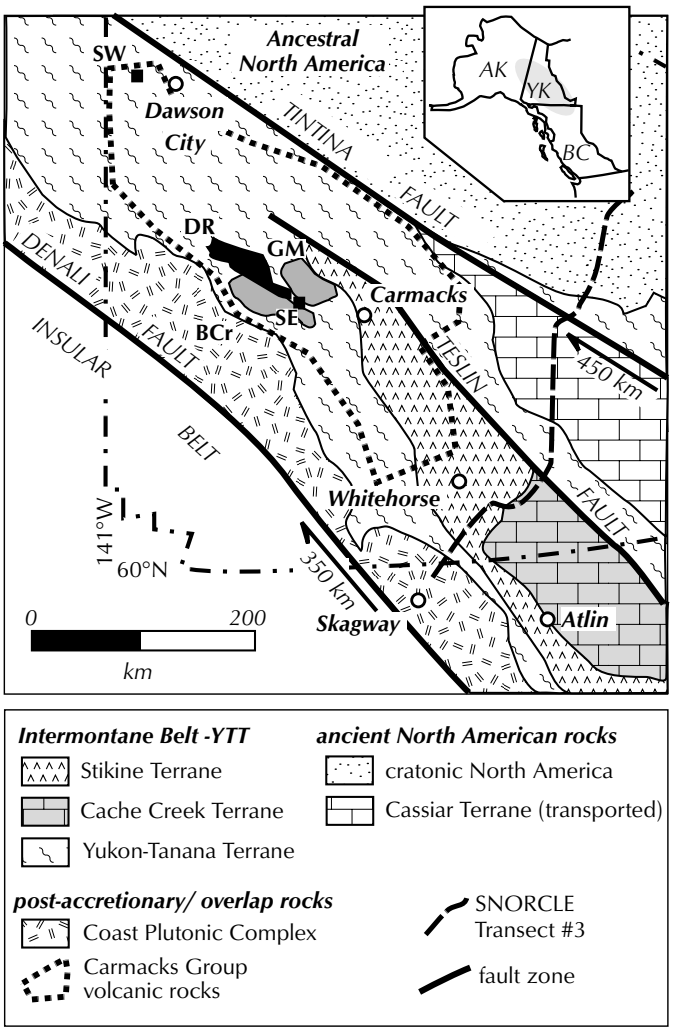

Figure 1. *Tectonic elements of the Northern Canadian Cordillera. Inset abbreviations are AK - Alaska; BC - British Columbia; and YK - Yukon. YTT units from which paleomagnetic studies are reported: BCr - 190 Ma Big Creek batholith; DR - 105 Ma Dawson Range batholith; GM - 190 Ma Granite Mountain batholith; SE - 69 Ma Seymour Creek stock; SW - 70 Ma Swede Dome stock. The extent of the 70 Ma Carmacks Group volcanic rocks is given by the dashed line.*

A complementary program of study is underway for the 'pericratonic' Yukon-Tanana Terrane (YTT) to discern its geotectonic motion history and to test its coherency since Early Jurassic time. The YTT is a poorly exposed assemblage of Paleozoic continental rocks with apparent North American affinity that underlies much of central Yukon and eastern Alaska. Its size, cratonic provenance and central position make the YTT a key tectonic element in the assembly of the Northern Cordillera (Fig. 1), but its past relations to other far-traveled terranes and to North America itself are poorly understood (Mortensen, 1992; Lowe et al., 1994). The YTT may have acted as a 'bumper' to halt the motions of other terranes in the Late Triassic (McClelland et al., 1992; Mihalynuk et al., 1994) or Eocene (Symons et al., 2000a), or it may have participated, at least in part, with other accreted terrane motions relative to North America (Irving et al., 1996; Johnston et al., 1996a).

Paleomagnetic results from the ~190 Ma Big Creek batholith of west-central Yukon indicate that the YTT has experienced minimal net latitudinal transport and counter-clockwise rotation with respect to North America since the Early Jurassic, a history that is markedly different from the significant poleward transport and clockwise rotations exhibited by Early Jurassic and younger units of the Stikine Terrane (Symons et al., 2000b). Paleomagnetic and geobarometric results from the nearby and similar-aged Granite Mountain batholith are presented here as a further exploration of YTT history since the Early Jurassic.

GEOLOGICAL SETTING

The Early Jurassic Granite Mountain batholith is a buff-weathering, melanocratic, biotite-hornblende granodiorite intrusion of ~600 km^2 extent, emplaced in schists and gneisses of the YTT (Fig. 2). Along with the nearby Big Creek and Minto batholiths, the Granite Mountain batholith is part of a regional ~800-km-long belt of Late Triassic to Early Jurassic calc-alkaline intrusions extending from west of Whitehorse to east-central Alaska, consistent with a continental arc setting within the YTT (Johnston et al., 1996b; Mortensen et al., 2000).

The Granite Mountain batholith is situated within a fault-bounded block of the YTT, adjacent to rocks of the Stikine Terrane in the northeast. The dip-slip Big Creek Fault forms the southwest limit of the Granite Mountain batholith and its YTT host rocks, separating them from the ~190 Ma Big Creek batholith and the mid-Cretaceous Dawson Range batholith. Across the southern boundary

of the Granite Mountain batholith, Late Cretaceous Carmacks Group volcanic rocks of Millers Ridge lie on the downthrown side of the Miller fault, with a vertical displacement of at least 800 m. To the northeast, along the Yukon River valley, Triassic volcanic breccia and tuff of the Lewes River Group (Stikine Terrane) is in contact with the batholith along the dextral Hoochekoo fault. The Granite Mountain batholith is intruded by dacite dykes related to the ~105 Ma Mt. Nansen Group volcanic rocks and by feeder dykes for the overlying basal andesite flows of the ~70 Ma Carmacks Group (Tempelman-Kluit, 1984).

Southeast and northwest of the map area depicted in Figure 2, the Big Creek and Hoochekoo fault traces appear to merge, although definitive relationships are obscured by overlying Carmacks Group volcanic flows (Tempelman-Kluit, 1984). Post-Carmacks Group motion history recorded by these northwest-trending faults is minimal, but mid- to Late-Cretaceous dextral displacement on the Big Creek fault was at least 20 km (Johnston, 1999). Johnston (1999) also documents kinematic evidence for a prior ductile history of the Big Creek fault as a shear zone that accommodated the mid-Cretaceous intrusion of the northwest-trending Dawson Range batholith, with a net dextral motion of ~65 km. These motions are not geotectonically significant, but may bear upon the Early Jurassic relationship between the coeval Granite Mountain and Big Creek batholiths, now adjacent across the Big Creek fault (Fig. 2).

Coarse (>5 mm) pink K-feldspar phenocrysts are a distinguishing feature of the batholith, in places defining a weak magmatic fabric. In the west and northwest of the study area, equally large hornblende phenocrysts impart a swarthy melanocratic appearance to the granodiorite, defining a northwest-trending magmatic fabric. In thin section, the mineral phases are fresh, including subhedral hornblende, K-feldspar and brown biotite. Fresh to mildly altered plagioclase is abundant. Quartz is ubiquitous and interstitial to the above phases. Accessory minerals are titanite, apatite, zircon and magnetite.

In the south part of the study area, sites 7 and 6 (Fig. 2) samples were from a Cretaceous andesite porphyry dyke and nearby host batholith, respectively, exposed in a roadside quarry. The dyke carries ~5 mm plagioclase phenocrysts set in a fine groundmass of microcline,

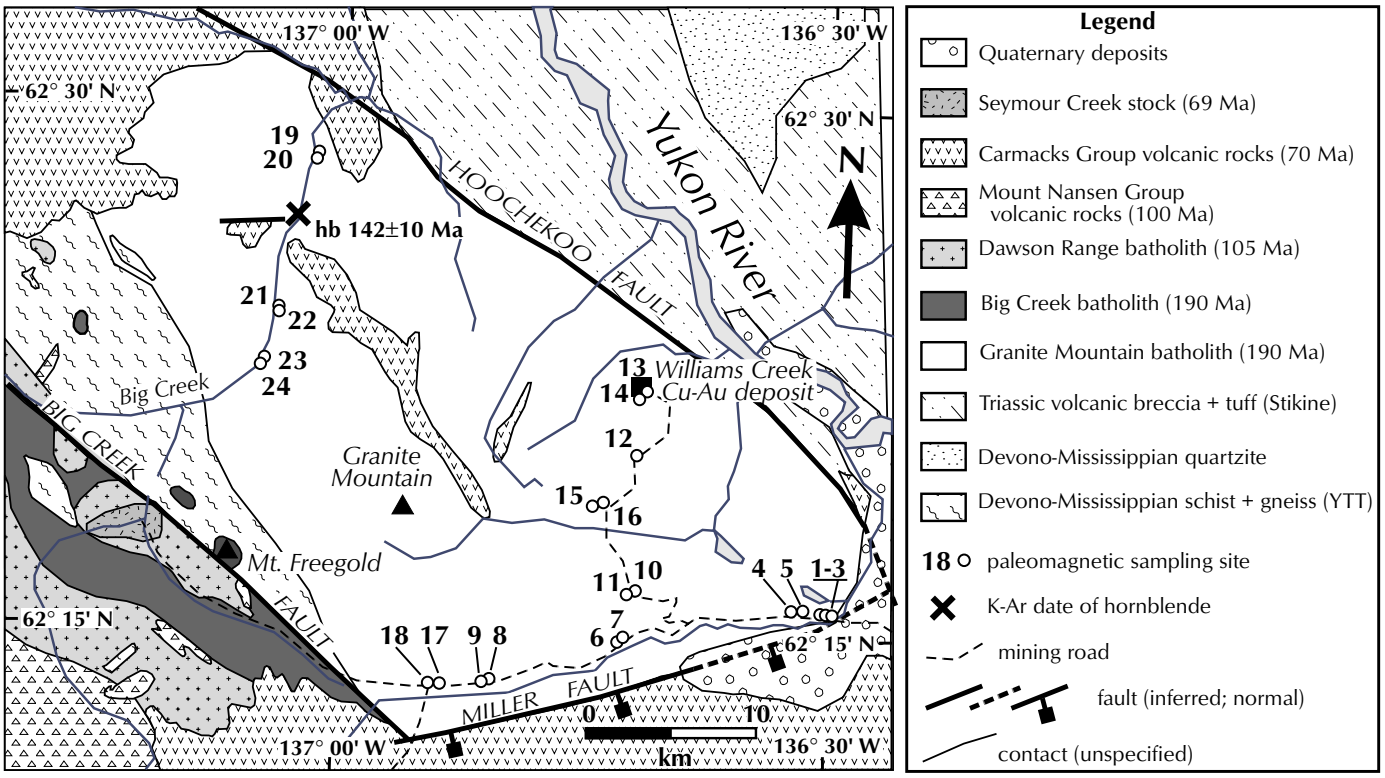

Figure 2. *Geology of the Granite Mountain batholith (after Tempelman-Kluit, 1984) including sampling sites.*

strongly altered plagioclase, interstitial chlorite, quartz, and well-distributed subangular iron-oxides. The dyke lacks the phenocrystic quartz that is typical of the mid-Cretaceous Mt. Nansen feeder dykes; it is most likely related to the Late Cretaceous Carmacks Group basal andesites (Smuk et al., 1997). Site 6 was sampled from a brittle, yellowed granodiorite that has undergone extensive alteration of hornblende and plagioclase, apparently in association with the dyke.

Hornblende from the northwest part of the batholith has given a K-Ar age of 142 ± 10 Ma (Stevens et al., 1982) that has likely undergone resetting. A U-Pb titanite age of ~190 Ma has been reported for the batholith, along with U-Pb zircon crystallization ages of ~194 Ma and ~193 Ma for associated gneisses hosting the deformed Minto and Williams Creek copper-gold porphyry deposits, respectively (Mortensen et al., 2000; Yukon MINFILE, 2001). The gneisses are enclosed within the batholith, possibly as roof pendants (Gordey and Makepeace, 2001). These age and geological relations imply that the Granite Mountain batholith was emplaced into the freshly deformed gneiss as the youngest magmatic product in an active shear zone. Magmatic fabric along the west margin of the batholith may indicate the nearby presence of the shear zone's northwesterly trending wall within the Early Jurassic continental magmatic arc.

PALEOMAGNETISM

A total of 331 specimens from 24 sites were collected along mining roads in the southern and eastern parts of the batholith, as well as by helicopter along Big Creek in the northwest (Fig. 2). Each site is represented by at least six 2.54-cm diameter cores, oriented in situ by solar and/or magnetic compass. Standard specimens of 2.20 cm length were sliced from each core. The specimens underwent thermal and alternating field (AF) stepwise demagnetization at the University of Windsor Paleomagnetics Laboratory using a Sapphire Instruments SI-4 AF demagnetizer, a Magnetic Measurements MMTD-80 thermal demagnetizer, and an automated Canadian Thin Films (CTF) DRM-420 cryogenic magnetometer. All measuring instruments are set inside a magnetically shielded room, which permits entry of only 0.2% of the Earth's ambient magnetic field intensity.

Measurement of the specimens' natural remanent magnetizations (NRM) showed a median intensity of 7.7×10^{-2} A/m (1st quartile, 5.0×10^{-2} A/m; 3rd quartile, 19.0×10^{-2} A/m). Specimen volume magnetic susceptibilities, measured with a Sapphire Instruments SI-2B magnetic susceptibility meter, had a median value of 10.0×10^{-3} SI (1st quartile, 6.6×10^{-3} SI; 3rd quartile, 18.0×10^{-3} SI). Both the NRM intensities and the bulk susceptibility values found here are normal for granodioritic rocks (e.g., Lowe et al., 1994).

After NRM measurement, two pilot specimens per site were thermally demagnetized in 13-16 steps up to at least 580°C, and two other pilot specimens were AF-demagnetized in 12 steps up to 130 mT. Thermal demagnetization of 48 pilot specimens revealed distributed unblocking, punctuated in some cases by an intensity drop in the 530°C-580°C range (Fig. 3), implying that magnetite carries the characteristic remanent magnetization (ChRM). Most specimens lost ~90% of their NRM intensity by 450°C, suggesting that multidomain magnetite is likely a significant remanence carrier. At several sites, specimens broke up in the oven at temperatures >470°C. AF step demagnetization removed a 'soft' viscous remanent magnetization (VRM) by ~15 mT, whereas thermal methods required ~260°C. VRM observed in both thermal and AF demagnetizations accounted for 50%-80% of the NRM intensity, and typically was directed steeply downwards to the north-northeast, consistent with its originating from the present Earth's magnetic field in Yukon. AF demagnetization beyond 30 mT commonly led to unstable remanence behaviour, implying the presence of multidomain magnetite.

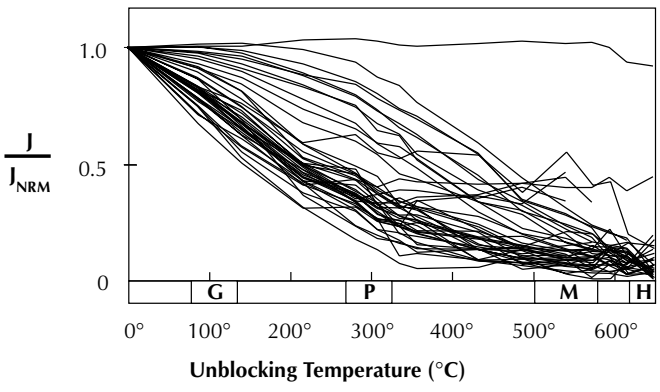

Figure 3. *Thermal demagnetization intensity decay curves for 48 pilot specimens from the Granite Mountain batholith. G, P, M, and H denote the characteristic unblocking temperature ranges of goethite, pyrrhotite, magnetite and hematite, respectively. J/J_{NRM} is the ratio of measured remanence intensity to the initial, NRM intensity.*

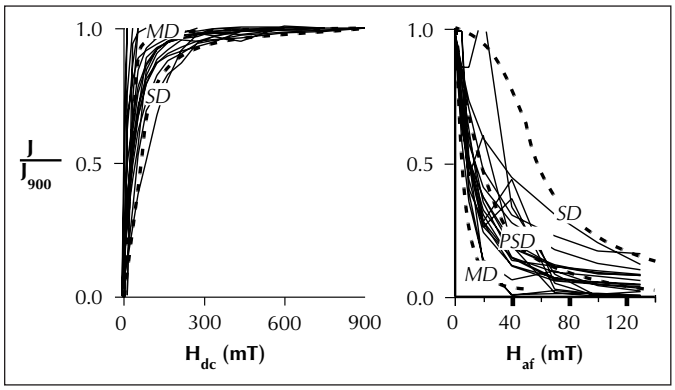

Figure 4. *Saturation isothermal remanent magnetization (SIRM) acquisition and decay curves for 19 specimens from the Granite Mountain batholith. Saturation remanence acquisition is plotted as intensity normalized to saturation intensity (J/J_{900}) versus direct field (H_{dc}) steps up to 900 mT, and remanence decay is plotted versus alternating-field (H_{af}) steps to 130 mT. Dashed curves are given for multidomain (MD), pseudo-single domain (PSD), and single-domain (SD) magnetite.*

Saturation isothermal remanent magnetization (SIRM) acquisition and decay curves were obtained for specimens from 19 sites using a Sapphire Instruments SI-6 pulse magnetizer by magnetizing them in 14 direct-field steps up to 900 mT, and then demagnetizing them in 7 AF steps up to 130 mT. The presence of pseudosingle to multidomain magnetite remanence carriers is confirmed by the generally rapid saturation and decay SIRM behaviour of the Granite Mountain specimens (Fig. 4).

The presence of multidomain magnetite is of concern since it can acquire a remanence at relatively low temperatures (~200°C), but may require laboratory unblocking temperatures of up to 450°C to remove significantly overlapping remanence information carried by pseudosingle and single domain magnetite (Dunlop and Argyle, 1991). Also, the significant presence of multidomain magnetite tends to contribute 'noise' to higher field steps during AF demagnetization (Dunlop and Ozdemir, 1997). To address this problem, 130 specimens were subjected to low-temperature demagnetization (LTD) in field-free space prior to stepwise thermal demagnetization, to remove the multidomain magnetite contribution to remanence (Dunlop and Argyle, 1991; Warnock et al., 2000). The remaining specimens in the collection were thermally demagnetized in steps starting from 450°C.

Specimens selected for LTD typically lost between 55% and 85% of their NRM intensities upon cycling through liquid Nitrogen temperature (95 K), thus matching in direction and intensity the remanence that is removed by 15 mT or 450°C. Accordingly, characteristic remanent magnetization (ChRM) directions are determined using specimens which were subjected to post-LTD thermal demagnetization, along with other specimens that exhibited stable remanence at unblocking temperatures of >450°C and coercivities of >15 mT. ChRM directions were identified using the least-squares line-fitting method over four or more consecutive AF or thermal steps (Kirschvink, 1980), with a maximum uncertainty of <15° for the fitted vector.

The paleomagnetic behaviour of specimens from the Granite Mountain batholith is complex (Fig. 5). North and west of the batholith, a ChRM **A** component with mean direction D=337, inclination I=69° (8 sites; α_{95}=7.6°; k=54.5) is present (Fig. 5a-c). Some **A** specimens (Fig. 5a) exhibit poor northwest and down ChRM directions, requiring the anchoring of the fitted vector to the zero remanence origin. A north-and-up ChRM **B** component with mean direction (D=024, I=-54°; α_{95}=14.0°, k=78.3) exists in three southeastern sites (Fig. 5d). The Cretaceous andesite porphyry dyke and its contact zone give a steep down remanence direction, **C** (Fig. 5e). ChRM components **A, B** and **C** are mutually exclusive. Specimens from 11 other sites either did not carry a stable remanence, or had inconsistent directions from sample to sample, possibly due to lightning strikes. Site mean paleomagnetic results are set out in Table 1 and depicted in Figure 6.

PALEODEPTH ESTIMATES

To be meaningful, paleomagnetic directions must be referenced to the paleohorizontal at the time of remanence acquisition. Estimates of paleohorizontal are usually obtained from bedded depositional strata, but this is not possible for massive crystalline intrusions. Instead, we employ the aluminum-in-hornblende geobarometer (Anderson and Smith, 1995) to estimate crystallization pressures and therefore emplacement depths at various locations in the batholith, thus providing a batholith-scale estimate of paleohorizontal at the time of emplacement.

Following petrographic inspection of a polished thin section from each site, 10 sites were chosen to represent the Granite Mountain batholith. Each chosen site contained the requisite mineral assemblage of amphibole,

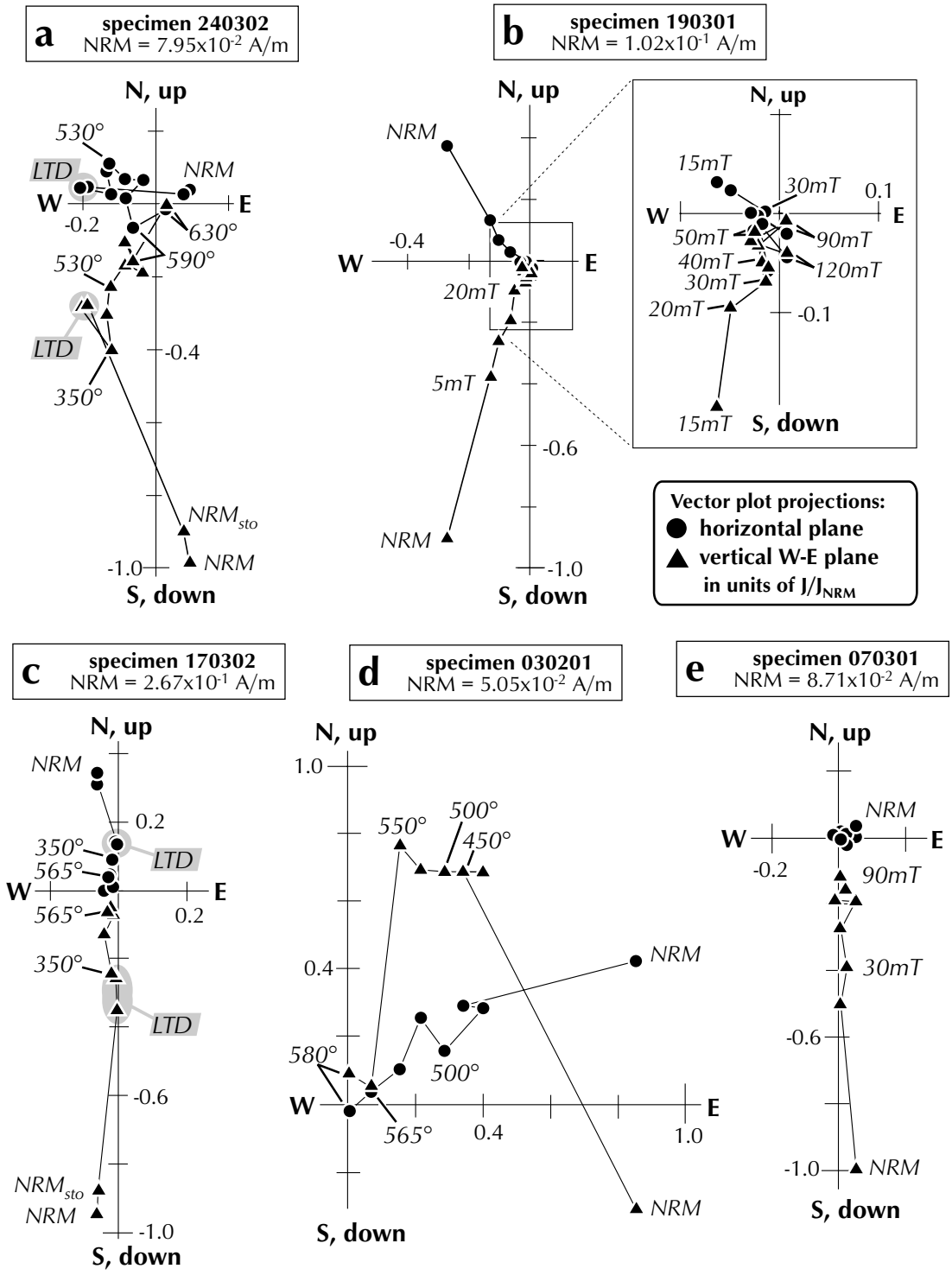

Figure 5. *NRM intensity-normalized orthogonal step demagnetization plots (Zijderveld, 1967) for representative specimens carrying the **A** remanence (a-c), the **B** remanence (d), and the **C** remanence (e). See text for discussion. NRM_{sto} is the natural remanent magnetization remaining in the specimen after decay during one year of storage in field-free space, prior to the stepwise demagnetization. LTD marks the low-temperature demagnetization steps discussed in the text. Circles mark the remaining remanence direction and intensity at each demagnetization step projected into the map-like horizontal north-south, east-west plane, whereas triangles mark the same stepwise demagnetization vectors projected into the vertical, east-west plane.*

plagioclase, K-feldspar, quartz, biotite, titanite, apatite, and magnetite or ilmenite, with minimal or no alteration of the primary igneous phases. It has been shown empirically (Hammarstrom and Zen, 1986) and experimentally (Schmidt, 1992) that the aluminum content in Ca-amphiboles increases linearly with greater pressure of crystallization under equilibrium H_2O-saturated conditions. Pressure estimates may be corrected for effect of temperature through the plagioclase-hornblende geothermometer (Blundy and Holland, 1990).

Electron microprobe elemental abundance analyses of two hornblende and plagioclase pairs in each site were performed using a JEOL JXA-8600 Superprobe at the University of Western Ontario, using standards as reported in Symons et al. (2000b). Analytical data were reduced for elemental abundances using structural formulae with 32 oxygens for plagioclase (Blundy and Holland, 1990), and by the ferric-iron maximizing method of Schumacher (1997) for amphibole. Plagioclase and amphibole were each analysed three to five times near their common boundaries for averaging and to test reproducibility. Within-crystal variation between analyses was typically less than 1% of the measured elemental abundances. Additionally, both the calcium (Ca) content in plagioclase and the aluminum (Al) content in hornblende are consistent between crystal pairs within each site (Table 2; Fig. 7). Plagioclase analyses range from An_{19} to An_{33}, within the calibrated limits of the geothermometer, and amphiboles are tschermakites to ferrotschermakites in the classification of Leake et al. (1997), with Al^{TOT} ranging from 1.8 to 2.1 atomic formula units (Table 2).

Initial pressure estimates (method of Schmidt, 1992), crystallization temperatures, and temperature-corrected pressure estimates for the 10 sites are given in Table 3. Emplacement depths, calculated assuming a baric gradient of 0.036 km/MPa (density 2.8 g/cm^3), and corrected for relative topographic differences between

Table 1. *Site mean remanence data for the Granite Mountain batholith, Yukon.*

Site[a]	n/N	ChRM Direction			
		Dec (°)	Inc (°)	α_{95} (°)	k
02[b]	6/15	024.2	-52.7	7.2	87.1
03[b]	11/13	021.8	-63.6	6.2	55.3
05[b]	5/12	025.3	-45.5	13.1	35.2
06[c]	11/15	258.1	81.6	7.6	36.9
07[c]	13/13	344.7	85.4	5.8	52.8
08	7/13	328.1	76.5	10.9	31.9
09	7/15	002.7	64.3	11.8	27.1
17	8/15	350.6	75.3	6.9	65.7
18	7/15	353.0	61.1	10.0	37.7
19	8/14	308.1	70.5	7.5	55.0
20	7/11	310.1	61.3	9.6	40.4
23	6/12	002.8	64.4	10.2	44.1
24	7/11	310.5	68.5	9.5	41.3
B =3 sites		024.0	-53.9	14.0	78.3
A=8 sites		336.8	69.4	7.6	54.5

[a]Sites 1, 4, 10-13, 15, 21 and 22 carry unstable remanence; sites 14, 16 carry stable remanence with inconsistent between-sample directions, probably due to lightning strike.

[b]Sites exhibiting **B** ChRM directions.

[c]Sites from a Cretaceous dyke and its contact zone, exhibiting **C** ChRM directions.

n/N: Number of specimens useable for site mean ChRM calculation/total number of specimens in site. Site mean ChRM directions are given by: Dec - declination; Inc - inclination; α_{95} - radius of 95% cone of confidence, and k - precision parameter.

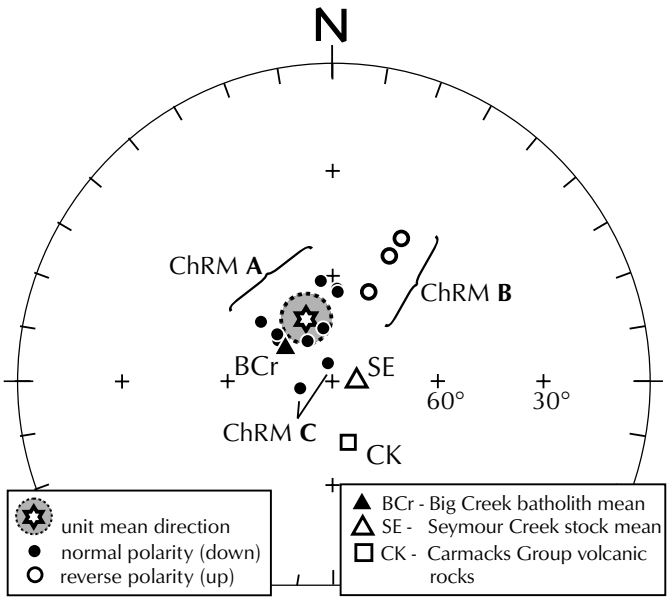

Figure 6. *Equal-area stereonet projection showing all site means from the Granite Mountain batholith (Table 1), along with reported mean direction for the Big Creek batholith (Symons et al., 2000b), the Seymour Creek stock (McCausland et al., 2001) and the Carmacks Group volcanic rocks (Wynne et al., 1998). Closed and open symbols represent down and up directions, respectively.*

Table 2. *Averaged amphibole analyses from the Granite Mountain batholith, using the structural formula calculation procedure of Schumacher (1997).*

	04-A	04-B	11-A	11-B	12-A	12-B	14-A	14-B	15-A	15-B
SiO_2 (wt.%)	40.46	40.67	41.07	40.94	41.81	41.52	41.13	40.94	40.73	41.23
TiO_2	0.91	0.91	0.96	1.05	0.94	0.78	0.61	0.73	0.91	0.9
Al_2O_3	11.48	11.23	11.21	11.34	10.51	10.8	11.09	11.11	11.56	11.58
Fe_2O_3*	4.75	4.29	4.73	4.94	4.25	4.32	4.66	4.5	4.89	4.09
Cr_2O_3	0.04	0.04	0.02	0.00	0.05	0.05	0.05	0.01	0.00	0.01
FeO	15.72	15.78	16.32	16.23	15.79	16.03	15.23	15.8	16	16.77
MnO	0.51	0.59	0.47	0.45	0.61	0.62	0.58	0.59	0.56	0.49
MgO	8.33	8.32	8.14	8.15	8.99	8.66	8.76	8.5	8.21	8.05
CaO	11.68	11.74	11.76	11.72	11.48	11.49	11.5	11.69	11.63	11.7
Na_2O	1.4	1.3	1.32	1.33	1.56	1.54	1.47	1.49	1.37	1.37
K_2O	1.41	1.37	1.24	1.26	1.29	1.33	1.31	1.33	1.45	1.38
H_2O*	1.88	1.88	1.91	1.9	1.91	1.91	1.9	1.89	1.9	1.92
F	0.05	0.04	0.02	0.04	0.03	0.00	0.02	0.04	0.03	0.01
Cl	0.07	0.05	0.06	0.04	0.07	0.07	0.05	0.03	0.05	0.04
Total	98.67	98.23	99.22	99.4	99.29	99.12	98.36	98.64	99.29	99.56
Si(cations)	6.256	6.308	6.314	6.284	6.401	6.379	6.351	6.323	6.263	6.317
$^{[4]}Al$	1.744	1.692	1.686	1.716	1.599	1.621	1.649	1.677	1.737	1.683
$^{[6]}Al$	0.347	0.362	0.345	0.335	0.297	0.333	0.369	0.347	0.357	0.408
Ti	0.106	0.107	0.111	0.122	0.108	0.09	0.07	0.084	0.105	0.104
Cr	0.005	0.004	0.002	0.001	0.006	0.006	0.006	0.002	0.00	0.002
Fe^{3+}	0.553	0.501	0.547	0.57	0.49	0.499	0.541	0.523	0.565	0.472
$^{[C]}Fe^{2}+$	2.032	2.047	2.098	2.083	2.022	2.059	1.967	2.04	2.057	2.149
$^{[C]}Mn$	0.037	0.055	0.033	0.025	0.025	0.03	0.03	0.047	0.034	0.026
Mg	1.92	1.924	1.865	1.864	2.052	1.983	2.017	1.957	1.881	1.839
$^{[B]}Mn$	0.031	0.023	0.029	0.034	0.054	0.051	0.046	0.031	0.039	0.037
$^{[B]}Fe^{2+}$	0.00	0.00	0.00	0.00	0.00	0.00	0.00	0.00	0.00	0.00
Ca	1.934	1.951	1.937	1.928	1.884	1.891	1.902	1.934	1.916	1.921
$^{[B]}Na$	0.035	0.026	0.034	0.038	0.062	0.058	0.052	0.035	0.045	0.042
$^{[A]}Na$	0.384	0.366	0.361	0.358	0.399	0.401	0.386	0.41	0.365	0.364
K	0.279	0.271	0.243	0.248	0.252	0.261	0.259	0.262	0.284	0.27
OH*	1.958	1.967	1.978	1.969	1.967	1.981	1.977	1.972	1.973	1.984
F	0.025	0.02	0.008	0.021	0.014	0.00	0.01	0.019	0.013	0.005
Cl	0.017	0.013	0.015	0.01	0.018	0.019	0.013	0.009	0.014	0.011
$Al_{[TOT]}$	2.091	2.054	2.031	2.052	1.896	1.955	2.018	2.023	2.094	2.092
Fe^{3+}#	0.214	0.197	0.207	0.215	0.195	0.195	0.216	0.204	0.216	0.18
Fe#	0.574	0.57	0.586	0.587	0.55	0.563	0.554	0.567	0.582	0.588

*Fe_2O_3 and H_2O are back-calculated from the structural formula. $Fe^{3+}\# = Fe^{3+}/(Fe^{3+} + Fe^{2+})$; $Fe\# = (Fe^{3+} + Fe^{2+})/(Fe^{3+} + Fe^{2+} + Mg)$.

(continued) ***Table 2.***

	09-A	09-B	18-A	18-B	20-A	20-B	21-A	21-B	23-A	23-B
SiO_2 (wt.%)	42.63	42.51	42.87	42.49	42.09	42.44	42.5	42.44	41.88	42.25
TiO_2	0.99	0.87	0.74	0.76	0.83	0.85	0.95	0.92	0.8	0.72
Al_2O_3	9.91	10.12	10.24	10.7	10.55	10.36	9.76	10.24	10.78	10.62
Fe_2O_3*	3.06	4.35	4.46	5.05	4.45	3.9	4.01	3.03	4.65	4.02
Cr_2O_3	0.07	0.07	0.04	0.01	0.01	0.01	0.02	0.03	0.01	0.02
FeO	14.54	14.1	12.93	12.73	13.64	14.09	14.68	15.22	13.13	13.51
MnO	0.52	0.52	0.64	0.63	0.47	0.51	0.49	0.47	0.59	0.45
MgO	10.06	10.02	10.48	10.41	10.04	10.03	9.84	9.68	10.17	10.26
CaO	11.82	11.79	11.89	11.95	11.68	11.77	11.67	11.77	11.87	11.87
Na_2O	1.31	1.31	1.18	1.21	1.32	1.34	1.33	1.42	1.29	1.31
K_2O	1.18	1.15	1.02	1.09	1.13	1.14	1.16	1.19	1.21	1.18
H_2O*	1.92	1.93	1.94	1.93	1.93	1.93	1.91	1.92	1.92	1.93
F	0.02	0.01	0.00	0.05	0.00	0.00	0.03	0.02	0.03	0
Cl	0.06	0.06	0.05	0.04	0.03	0.05	0.05	0.04	0.04	0.04
Total	98.11	98.81	98.48	99.05	98.19	98.42	98.4	98.4	98.35	98.2
Si (cations)	6.532	6.475	6.506	6.424	6.436	6.478	6.512	6.502	6.394	6.45
$^{[4]}Al$	1.468	1.525	1.494	1.576	1.564	1.522	1.488	1.498	1.606	1.55
$^{[6]}Al$	0.322	0.291	0.337	0.331	0.338	0.342	0.274	0.351	0.334	0.362
Ti	0.114	0.1	0.085	0.086	0.096	0.097	0.11	0.106	0.091	0.083
Cr	0.009	0.008	0.005	0.001	0.002	0.001	0.003	0.003	0.001	0.003
Fe^{3+}	0.353	0.499	0.509	0.575	0.512	0.448	0.462	0.35	0.534	0.462
$^{[C]}Fe^{2+}$	1.863	1.796	1.641	1.609	1.744	1.798	1.881	1.95	1.676	1.725
$^{[C]}Mn$	0.04	0.032	0.052	0.051	0.02	0.031	0.024	0.03	0.05	0.031
Mg	2.299	2.275	2.371	2.347	2.288	2.283	2.247	2.211	2.315	2.334
$^{[B]}Mn$	0.028	0.036	0.031	0.03	0.04	0.035	0.04	0.031	0.027	0.027
$^{[B]}Fe^{2+}$	0.00	0.00	0.00	0.00	0.00	0.00	0.00	0.00	0.00	0
Ca	1.941	1.923	1.934	1.936	1.914	1.925	1.915	1.933	1.942	1.942
$^{[B]}Na$	0.032	0.041	0.035	0.034	0.046	0.04	0.045	0.036	0.031	0.031
$^{[A]}Na$	0.358	0.346	0.312	0.32	0.346	0.355	0.349	0.386	0.351	0.358
K	0.231	0.224	0.197	0.211	0.22	0.222	0.227	0.233	0.235	0.231
OH*	1.976	1.978	1.987	1.968	1.992	1.986	1.971	1.98	1.974	1.987
F	0.008	0.005	0.00	0.023	0.00	0.00	0.015	0.009	0.015	0.001
Cl	0.016	0.016	0.013	0.009	0.008	0.014	0.014	0.011	0.01	0.011
$Al_{[TOT]}$	1.79	1.816	1.831	1.907	1.902	1.864	1.763	1.849	1.94	1.911
Fe^{3+}#	0.159	0.217	0.237	0.263	0.227	0.199	0.197	0.152	0.242	0.211
Fe#	0.491	0.502	0.476	0.482	0.497	0.496	0.51	0.51	0.488	0.484

sites, define two domains in the batholith (Table 3; Fig. 8): 16.1 ± 0.5 km in the north and west (five sites), and 18.8 ± 0.6 km to the southeast (five sites). Topographic correction is minor, as all sites occur within a 0.5-km-range of elevation. The paleodepth estimates imply either a west ~6° tilt of a coherent intrusive body, or more likely, a subdivision of the batholith into at least two blocks, which experienced differential uplift.

Table 3. *Site-averaged compositions of co-existing amphibole and plagioclase crystal pairs and consequent thermobarometric data for the Granite Mountain batholith.*

Site pair	Plag An#	Amph Al[TOT]	P-Sch (MPa)	Temp (°C)	P-A&S (MPa)	Depth (km)	Corr. Depth (km)
04-A	24.9	2.09	703	769	523	18.6	18.6
04-B	25.4	2.05	685	762	526	18.7	18.7
11-A	26.2	2.03	674	764	509	18.1	18.3
11-B	27.0	2.05	684	771	502	17.8	18.0
12-A	19.5	1.90	609	739	507	18.0	18.2
12-B	19.7	1.96	638	739	532	18.9	19.1
14-A	22.2	2.02	668	746	545	19.4	19.5
14-B	22.8	2.02	671	754	531	18.9	19.0
15-A	26.5	2.09	705	769	524	18.6	18.8
15-B	25.5	2.09	704	756	555	19.7	19.9
09-A	29.6	1.79	558	746	446	15.9	16.2
09-B	30.1	1.82	571	758	433	15.4	15.7
18-A	32.7	1.83	578	757	442	15.7	16.1
18-B	32.6	1.91	615	769	446	15.9	16.2
20-A	31.1	1.90	612	762	461	16.4	16.3
20-B	32.0	1.86	594	758	452	16.1	15.9
21-A	28.9	1.76	545	750	426	15.1	15.1
21-B	28.6	1.85	587	745	473	16.8	16.8
23-A	31.5	1.94	630	769	459	16.3	16.3
23-B	31.3	1.91	617	758	473	16.8	16.8
East	24.0	2.03	670	757	525	18.7	18.8
s.d.	±2.6	±0.06	±29	±12	±16	±0.6	±0.6
West	30.8	1.86	591	757	451	16.0	16.1
s.d.	±1.4	±0.06	±27	±8	±15	±0.5	±0.5

Notes: Plagioclase An# - the atomic ratio [Ca/(Na+Ca+K)]; Amphibole Al[TOT] - the average total number of Al cations calculated in the structural formula (Table 2); P-Sch - pressure calculated using Schmidt (1992); Temp - temperature calculated using the plagioclase-amphibole geothermometer of Blundy and Holland (1992); P-A&S - the final temperature-corrected pressure estimate, calculated using Anderson and Smith (1995); Corr. Depth - paleodepth estimates that have been corrected for minor variation in present-day topography, with the correction made arbitrarily to the elevation at site 4.

Within each domain, the paleodepth estimates are consistent with present horizontal, given the relative uncertainty of the method (±0.5 km, Anderson and Smith, 1995). The depth difference between western and eastern domains therefore suggests the presence of a roughly north-northwest-trending normal fault separating the domains, with ~2.5 km east-side-up displacement. The eastern portion of the batholith may be a 'pop up' sliver, involving a west-side-up displacement on the Hoochekoo Fault. Alternatively, the ~2.5 km depth difference between domains may mark an original difference in intrusive depth between two phases of the batholith, emplaced at slightly different times.

Crystal-pair plagioclase Ca content and amphibole Al content differs markedly between western and eastern sites of the batholith (Fig. 7). Such a bimodal distribution suggests that geobarometric comparisons between the batholith domains should be made with caution; it is as if they were separate intrusions. Paleodepth estimates from the two domains almost agree within the geobarometric method's ±2 km absolute uncertainty (Anderson and Smith, 1995), which is partly based on the compositional variation amongst the intrusions used to calibrate the geobarometer (Hammarstrom and Zen, 1986). Nevertheless, the sense of depth difference between western and eastern batholith domains is probably correct.

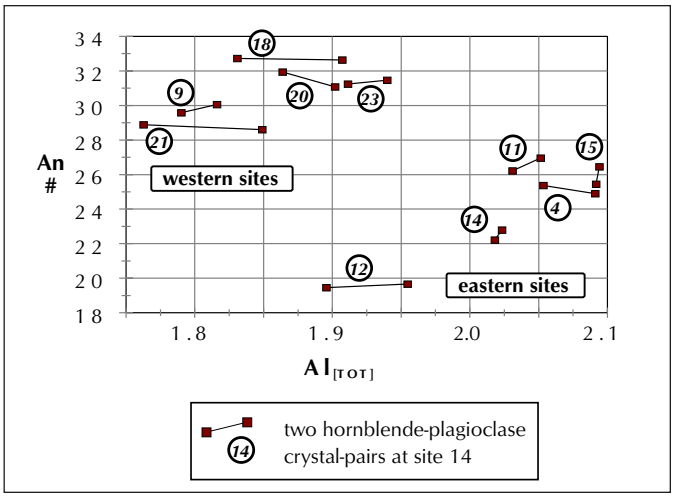

Figure 7. *Plagioclase and hornblende crystal-pairs for each site plotted as calcium content in plagioclase (Anorthite # - An #) versus total number of aluminum cations ($Al_{[TOT]}$) in hornblende. Within-site consistency is indicated by the similarity of pairs from each site.*

DISCUSSION

Given the estimated emplacement depths of 16-19 km, the ambient post-emplacement temperatures would have been >480°C (assuming ~30°/km geothermal gradient), too high for an enduring remanence to be acquired by magnetite (Pullaiah et al., 1975). Any ChRM present was likely recorded during uplift through ~15 km depth. Simple time-linear uplift of the batholith from 16-19 km at 190 Ma to surfacing, and deposition of the Carmacks Group flows at 70 Ma, indicates that the **A** and **B** ChRMs would have been acquired at 180-170 Ma. Rapid early uplift is also suggested by cooling curves obtained from the coeval Aishihik batholith to the south (Johnston et al., 1996b).

Remanence **C** is younger, related to the emplacement of the Cretaceous andesite dyke. The westerly, steep-down ChRM compares well with the ChRM recovered from 14 reversed- and 2 normal-polarity sites of the nearby 69 Ma Seymour Creek stock (McCausland et al., 2001). Alternatively, the ChRM **C** is similar to the nearly vertical-down ChRM directions found in a preliminary analysis of the 105 Ma Dawson Range batholith (McCausland et al., 2000a), although the dyke appears to be younger, and is likely a feeder for the overlying 70 Ma Carmacks andesite flows.

Remanence **B** has no clear tectonic meaning, with its direction plotting well away from the antipode to **A**, or any possible North American reference pole. It is resolved in only three sites, all sampled by road from the southeasternmost part of the Granite Mountain batholith, where the Miller and Hoochekoo faults meet (Fig. 8). The **B** ChRM direction may be resident in a local, tumbled block of km size, marking the fault-bounded corner of the exposed batholith.

Unlike ChRM **B**, the **A** ChRM is observed in eight sites distributed across the western and northern portions of the batholith. Its wide geographic distribution is coincident with the sites that show geobarometric depth estimates of ~16 km, strongly indicating that no tilt correction of the **A** ChRM direction is required. Remanence **A** gives a paleopole position of 74.7°N, 106.9°E (dp=11°, dm=13°), which has negligible rotation and is 690 km ± 1090 km near-sided compared with the 180 Ma North American reference pole of Besse and

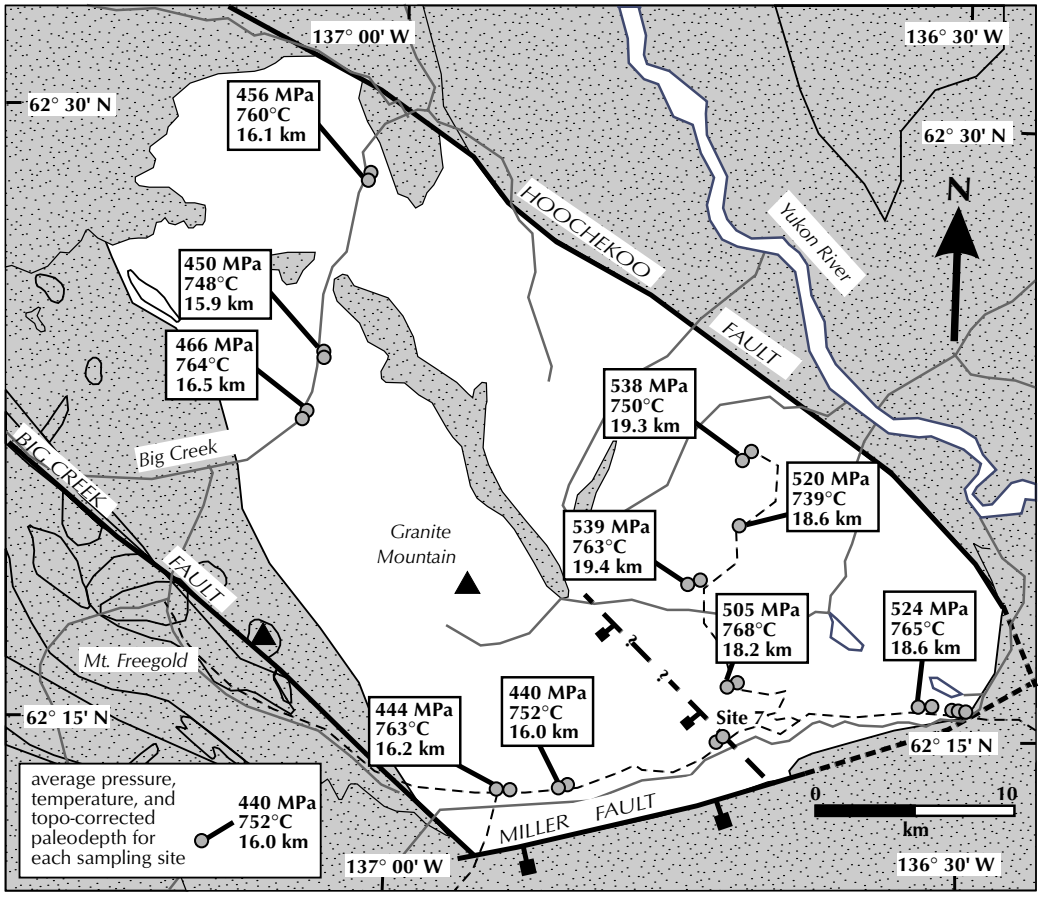

Figure 8. *Pressure, temperature and intrusion depth estimates for the Granite Mountain batholith. A possible normal fault between eastern and western portions of the batholith is marked by a dashed line. Note that such a fault might have provided a conduit for the 70 Ma Carmacks Group magmatism preserved along the centre of the batholith and as a dyke at Site 7.*

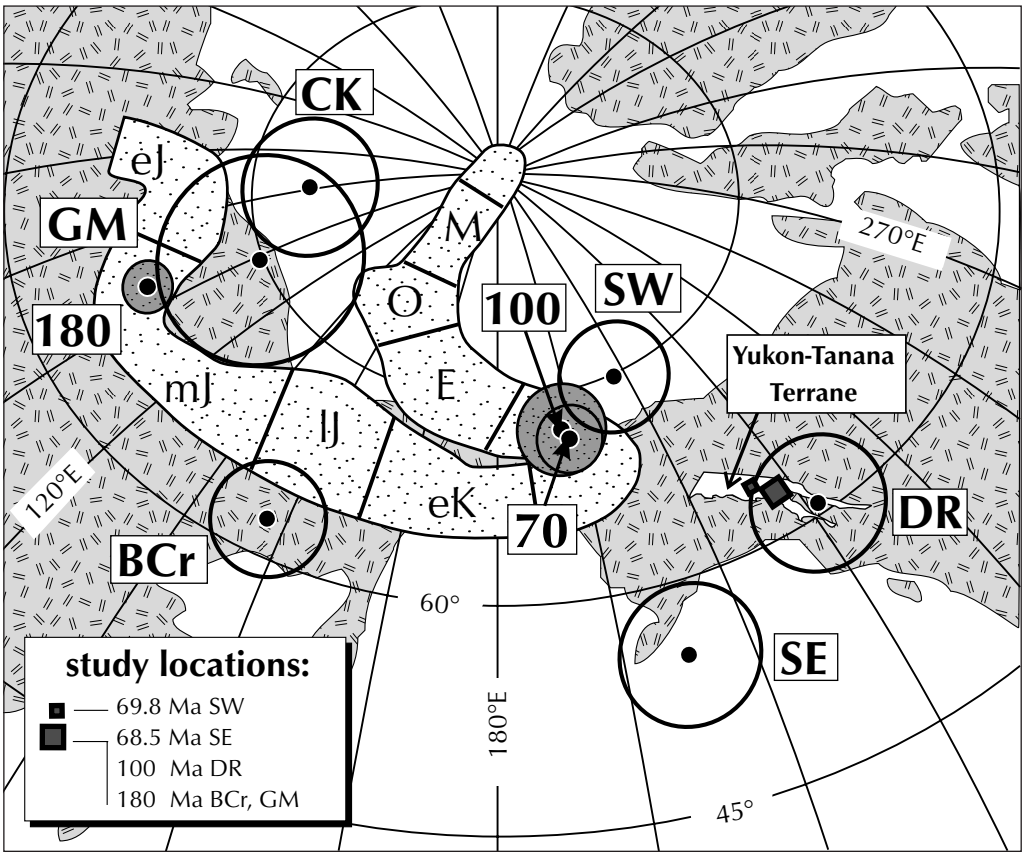

Figure 9. *YTT paleopoles and their 1-sigma confidence ellipses plotted on the present-day globe with reference to the North American apparent polar wander path (stippled pattern) of Besse and Courtillot (1991), from Early Jurassic (eJ) time to the present day, with its 1-sigma bounds. CK - 70 Ma Carmacks Group volcanic rocks; mJ – Middle Jurassic; lJ – Late Jurassic; eK – Early Cretaceous; E – Eocene; O – Oligocene; M – Miocene; all other abbreviations are defined in Figure 1. See text for discussion.*

Courtillot (1991). Both **A** and **C** remanence directions are similar to those expected for Early Jurassic and Late Cretaceous North American reference poles, respectively, and are most simply interpreted as representing minimal motion of the Granite Mountain batholith relative to North America since Early Jurassic time.

All paleomagnetic results reported to date for the YTT (Table 4) are plotted in Figure 9 as paleopoles with reference to a path of past positions of the North American pole (Besse and Courtillot, 1991). Results reported here for the Granite Mountain batholith are similar to those obtained from the Early Jurassic Big Creek batholith which carries a dual-polarity uplift remanence direction in 18 sites (Symons et al., 2000b). The much larger 1σ formal error ellipse of the Granite Mountain paleopole position mainly reflects its derivation from only eight sites.

Unlike the counter-clockwise-rotated Big Creek batholith, the Granite Mountain batholith result implies no significant net rotation with respect to North America since 180 Ma. Following this observation, it would appear that the Big Creek batholith has undergone 31° ± 19° of counter-clockwise rotation with respect to the Granite Mountain batholith at some time during their history, perhaps during motion along the Big Creek fault/shear zone that brought them into their current adjacency. Note

Table 4. *Net tectonic motion estimates from units of the YTT*[a].

Unit[b]	Age (Ma)	Paleopole Lat.(°N)	Paleopole Long.(°E)	A_{95}	Net Transport, Poleward[c];	Rotation Clockwise
GM	180	74.7°	106.9°	12.0°	-6.2°±9.8°;	4°±17°
BCr	180	62.9°	146.6°	6.5°	-10.1°±5.6°;	-27°±10°
DR[d]	105	61.1°	226.3°	8.1°	-12.3°±7.8°;	N/A
CK	70	78.4°	088.6°	7.8°	21.0°±7.0°;	22°±16°
SW[e]	70	77.3°	224.7°	6.0°	0.5°±5.8°;	44°±27°
SE	69	55.2°	202.5°	8.4°	-2.4°±7.5°;	-79°±36°

[a]Calculated with respect to North America paleopoles from Besse and Courtillot (1991): 180 Ma, 68.1°N, 101.2°E; A_{95}=2.7°; 100 Ma, 72.9°N, 191.4°E; A_{95}=5.4°; 70 Ma, 72.3°N, 192.7°E; A_{95}=4.1°.

[b]Unit abbreviations are defined in Figure 1.

[c]One degree of transport is equal to approximately 111 km.

[d]Dawson Range batholith (McCausland et al., 2000a).

[e]Swede Dome stock (McCausland et al., 2000b).

that the paleopoles also nonsignificantly imply that at 180 Ma, the Big Creek batholith was located in present-day coordinates, some 430 km ± 1200 km 'northwestwards' of the Granite Mountain batholith, requiring a net 'sinistral' motion to bring them to their present day positions. This apparent sinistral motion history is poorly resolved, but, if true, would have occurred prior to the mid-Cretaceous emplacement of the Dawson Range batholith, after which only minimal fault motions are known for the area (Johnston, 1999).

The Granite Mountain batholith paleopole overlaps that of the Late Cretaceous Carmacks Group volcanic rocks of Wynne et al. (1998), and the **A** ChRM may instead have been acquired during a thermal or hydrothermal event related to the overlying Carmacks volcanism at 70 Ma (Fig. 2). Evidence is lacking, however, for thermal paleomagnetic overprinting or hydrothermally driven creation of new magnetic material in sites carrying the **A** ChRM. The **A** remanence defined in this study unblocks at temperatures >450°C with no trace of another, higher temperature ancient component. In thin section, plagioclase shows only patchy alteration, with little or no alteration of hornblende. A pervasive hydrothermal event (Wynne et al., 1998) might be expected to produce extensive alteration along grain boundaries, a feature not observed for most sites of the Granite Mountain batholith.

Paleomagnetic results from the Granite Mountain batholith are most consistent with, but not rigorously supportive of, theories which postulate minimal tectonic motion for the YTT relative to North America since the Early Jurassic. Remanence **A** is not as well constrained as the dual-polarity results from the Big Creek batholith (Symons et al., 2000b). Additionally, the dyke- and contact-borne remanence **C** is not likely to have averaged out paleosecular variation of the Earth's magnetic field.

A major issue for future discussion is the poor agreement between the Carmacks Group paleomagnetism, which implies ~2000 km of polewards transport for the YTT and Stikine terranes since 70 Ma (Johnston et al., 1996a; Wynne et al., 1998), and paleomagnetic results from YTT intrusions, especially of 70 Ma age, which all imply minimal transport of the YTT from Early Jurassic to Eocene time (Symons et al., 2000a,b; McCausland et al., 2000a,b; 2001). Forthcoming results from other Jurassic, Cretaceous and Eocene units, along with a regional geological synthesis should further illuminate the YTT's motion history.

ACKNOWLEDGEMENTS

The authors express their gratitude to the Yukon Geology Program for essential assistance in this study. Harmen Keiser of Trans North Air provided safe and efficient helicopter support. Rachel Comber did measurements of magnetic susceptibility. Steve Johnston, Carmel Lowe, Currie Palmer and Maurice Colpron offered helpful discussions, and Yves Thibault provided guidance with the electron microprobe. The authors acknowledge financial support from LITHOPROBE-SNorCLE to DTAS and the Ontario Government Scholarship for Science and Technology to P. McCausland. This is also known as LITHOPROBE contribution #1265.

REFERENCES

Anderson, J.L. and Smith, D.R., 1995. The effects of temperature and f_{O_2} on the Al-in-hornblende barometer. American Mineralogist, vol. 80, p. 549-559.

Besse, J. and Courtillot, V., 1991. Revised and synthetic apparent polar wander paths of the African, Eurasian, North American and Indian Plates, and true polar wander since 200 Ma. Journal of Geophysical Research, vol. 96, p. 4029-4050.

Blundy, J.D. and Holland, T.J.B., 1990. Calcic amphibole equilibria and a new amphibole-plagioclase geothermometer. Contributions to Mineralogy and Petrology, vol. 104, p. 208-224.

Dunlop, D.J. and Argyle, K.S., 1991. Separating multidomain and single-domain-like remanences in pseudo-single-domain magnetites (215-540 nm) by low-temperature demagnetization. Journal of Geophysical Research, vol. 96, p. 2007-2017.

Dunlop, D.J. and Ozdemir, O., 1997. Rock Magnetism: Fundamentals and Frontiers. Cambridge Studies in Magnetism, Cambridge University Press, 573 p.

Gordey, S.P. and Makepeace, A.J. (comps.), 2001. Bedrock Geology, Yukon Territory. Geological Survey of Canada, Open File 3754 and Exploration and Geological Services Division, Yukon Region, Indian and Northern Affairs Canada, Open File 2001-1, 1:1 000 000 scale map.

Hammarstrom, J.M. and Zen, E., 1986. Aluminum in hornblende: an empirical igneous geobarometer. American Mineralogist, vol. 71, p. 1297-1313.

Harris, M.J., Symons, D.T.A., Blackburn, W.H. and Hart, C.J.R., 1999. Paleomagnetic and geobarometric study of the Late Cretaceous Mount Lorne stock, southern Yukon Territory. Canadian Journal of Earth Sciences, vol. 36, p. 905-915.

Irving, E., Wynne, P.J., Thorkelson, D.J. and Schiarizza, P., 1996. Large (1000 to 4000 km) northward movements of tectonic domains in the northern Cordillera, 83 to 45 Ma. Journal of Geophysical Research, vol. 101, p. 17901-17916.

Johnston, S.T., 1999. Large-scale coast-parallel displacements in the Cordillera: a granitic solution to a paleomagnetic dilemma. Journal of Structural Geology, vol. 21, p. 1103-1108.

Johnston, S.T., Wynne, P.J., Francis, D., Hart, C.J.R., Enkin, R.J. and Engebretson, D.C., 1996a. Yellowstone in Yukon: the Late Cretaceous Carmacks Group. Geology, vol. 24, p. 997-1000.

Johnston, S.T., Mortensen, J.K. and Erdmer, P., 1996b. Igneous and metaigneous age constraints for the Aishihik metamorphic suite, southwest Yukon. Canadian Journal of Earth Sciences, vol. 33, p. 1534-1555.

Kirschvink, J.L., 1980. The least squares line and plane and the analysis of paleomagnetic data. Geophysical Journal of the Royal Astronomical Society, vol. 62, p. 699-718.

Leake, B.E. (chairperson) et al., 1997. Nomenclature of amphiboles: report of the Subcommittee on Amphiboles of the International Mineralogical Association, Commission on New Minerals and Mineral Names. Canadian Mineralogist, vol. 35, p. 219-246.

Lowe, C., Horner, R.B., Mortensen, J.K., Johnston, S.T. and Roots, C.F., 1994. New geophysical data from the northern Cordillera: preliminary interpretations and implications for the tectonics and deep geology. Canadian Journal of Earth Sciences, vol. 31, p. 891-904.

McCausland, P.J.A., Symons, D.T.A., Hart, C.J.R. and Blackburn, W.H., 2000a. Minimal geotectonic motion of the Yukon-Tanana Terrane relative to North America: Preliminary paleomagnetic results from the Dawson Range batholith. LITHOPROBE, Slave-Northern Cordillera Lithospheric Evolution (SNorCLE) and Cordilleran Tectonics Workshop, Report of the Combined Meeting, Calgary, Alberta, LITHOPROBE Report 72, p. 146-154.

McCausland, P.J.A., Symons, D.T.A., Hart, C.J.R. and Blackburn, W.H., 2000b. Minimal geotectonic motion of the Yukon-Tanana Terrane relative to North America: Preliminary paleomagnetic results from two Late Cretaceous intrusions. GeoCanada 2000, Calgary, Alberta.

McCausland, P.J.A., Symons, D.T.A., Hart, C.J.R. and Blackburn, W.H., 2001. Paleomagnetic study of the Late Cretaceous Seymour Creek stock, Yukon: Minimal geotectonic motion of the Yukon-Tanana Terrane. *In:* Yukon Exploration and Geology 2000, D.S. Emond and L.H. Weston (eds.), Exploration and Geological Services Division, Yukon Region, Indian and Northern Affairs Canada, p. 207-216.

McClelland, W.C., Gehrels, G.E. and Saleeby, J.B., 1992. Upper Jurassic-Lower Cretaceous basinal strata along the Cordilleran Margin*:* Implications for the accretionary history of the Alexander-Wrangellia-Peninsular Terrane. Tectonics, vol. 11, no. 4, p. 823-835.

Mihalynuk, M.G., Nelson, J. and Diakow, L.J., 1994. Cache Creek terrane entrapment: oroclinal paradox within the Canadian Cordillera. Tectonics, vol. 13, no. 2, p. 575-595.

Mortensen, J.K., 1992. Pre-Mid-Mesozoic tectonic evolution of the Yukon-Tanana Terrane, Yukon and Alaska. Tectonics, vol. 11, no. 4, p. 836-853.

Mortensen, J.K., Emon, K., Johnston, S.T. and Hart, C.J.R., 2000. Age, geochemistry, paleotectonic setting and metallogeny of Late Triassic-Early Jurassic intrusions in the Yukon and eastern Alaska: A preliminary report. *In:* Yukon Exploration and Geology 2000, D.S. Emond and L.H. Weston (eds.), Exploration and Geological Services Division, Yukon Region, Indian and Northern Affairs Canada, p. 139-144.

Pullaiah, G.E., Irving, E., Buchan, K.L. and Dunlop, D.J., 1975. Magnetization changes caused by burial and uplift. Earth and Planetary Science Letters, vol. 28, p. 133-143.

Schmidt, M.W., 1992. Amphibole composition in tonalite as a function of pressure and experimental calibration of the Al-in-hornblende barometer. Contributions to Mineralogy and Petrology, vol. 110, p. 304-310.

Schumacher, J.C., 1997. The estimation of the proportion of ferric iron in the electron-microprobe analysis of amphiboles. Canadian Mineralogist, vol. 35, p. 238-246 (Appendix 2).

Smuk, K.A., Williams-Jones, A.E. and Francis, D., 1997. The Carmacks hydrothermal event: an alteration study in the southern Dawson Range, Yukon. *In:* Yukon Exploration and Geology 1996, Exploration and Geological Services Division, Yukon Region, Indian and Northern Affairs Canada, p. 92-106.

Stevens, R.D., DeLabio, R.N. and LaChance, G.R., 1982. Age determinations and geological studies, K-Ar isotopic ages. Geological Survery of Canada, Report 15, p 74.

Symons, D.T.A., Harris, M.J., Gabites, J.E. and Hart, C.J.R., 2000a. Eocene (51 Ma) end to northward translation of the Coast Plutonic Complex: paleomagnetism and K-Ar dating of the White Pass Dikes. Tectonophysics, vol. 326, p. 93-109.

Symons, D.T.A., Williams, P.R., McCausland, P.J.A., Harris, M.J., Hart, C.J.R. and Blackburn, W.H., 2000b. Paleomagnetism and geobarometry of the Big Creek Batholith suggests that Yukon-Tanana Terrane has been a parautochthon since Early Jurassic. Tectonophysics, vol. 326, p. 57-72.

Tempelman-Kluit, D.J., 1984. Geology of Laberge (105E) and Carmacks (115I) map areas, Yukon. Geological Survey of Canada, Open File 1101.

Warnock, A.C., Kodama, K.P. and Zeitler, P.K., 2000. Using thermochronology and low-temperature demagnetization to accurately date Precambrian paleomagnetic poles. Journal of Geophysical Research, vol. 105, no. B8, p. 19435-19453.

Wynne, P.J., Enkin, R.J., Baker, J., Jojnston, S.T. and Hart, C.J.R., 1998. The big flush: paleomagnetic signature of a 70 Ma regional hydrothermal event in displaced rocks of the northern Canadian Cordillera. Canadian Journal of Earth Sciences, vol. 35, p. 657-671.

Zijderveld, J.D.A., 1967. A.C. demagnetization of rocks: analysis of results. *In:* Methods in Paleomagnetism, D.E.W. Collinson, K.K. Crier and S.K. Runcorn (eds.), Elsevier, Amsterdam, The Netherlands, p. 254-286.